

Oxygen from the $\lambda 7774$ High-Excitation Triplet in Open Cluster Dwarfs: Hyades^{1,2}

Simon C. Schuler AND Jeremy R. King

Department of Physics and Astronomy, Clemson University

118 Kinard Laboratory, Clemson, SC, 29634

`sschule,jking2@ces.clemson.edu`

Donald M. Terndrup AND Marc H. Pinsonneault

Department of Astronomy, The Ohio State University

140 West 18th Avenue, Columbus, OH, 43210

`terndrup,pinsono@astronomy.ohio-state.edu`

Norman Murray

Canadian Institute for Theoretical Astrophysics, University of Toronto

60 St. George Street, Toronto, ON, M5S3H8, Canada

`murray@cita.utoronto.ca`

and

L.M. Hobbs

University of Chicago

Yerkes Observatory, Williams Bay, WI, 53191

`hobbs@yerkes.uchicago.edu`

¹Based on observations obtained with the Mayall 4-m telescope at Kitt Peak National Observatory, a division of the National Optical Astronomy Observatories, which is operated by the Association of Universities for Research Astronomy, Inc. under cooperative agreement with the National Science Foundation.

²This paper includes data taken with the Harlan J. Smith 2.7-m telescope at The McDonald Observatory of the University of Texas at Austin.

ABSTRACT

Oxygen abundances have been derived from the near-IR, high-excitation $\lambda 7774$ O I triplet in high-resolution, high signal-to-noise spectra of 45 Hyades dwarfs using standard one dimensional, plane-parallel LTE models. Effective temperatures of the stellar sample range from 4319 – 6301 K, and the derived relative O abundances as a function of T_{eff} evince a trichotomous morphology. At $T_{\text{eff}} > 6100$ K, there is evidence of an increase in the O abundances with increasing T_{eff} , consistent with non-LTE (NLTE) predictions. At intermediate T_{eff} ($5450 \leq T_{\text{eff}} \leq 6100$ K), the O abundances are flat, and star-to-star values are in good agreement, having a mean value of $[\text{O}/\text{H}] = +0.25 \pm 0.02$; however, systematic errors at the $\lesssim 0.10$ dex level might exist. The O abundances for stars with $T_{\text{eff}} \leq 5450$ K show a striking increase with *decreasing* T_{eff} , in stark contrast to expectations and canonical NLTE calculations. The cool Hyades triplet results are compared to those recently reported for dwarfs in the Pleiades cluster and the UMa moving group; qualitative differences between the trends observed in these stellar aggregates point to a possible age-related diminution of triplet abundance trends in cool open cluster dwarfs. Correlations with age-related phenomena, i.e., chromospheric activity and photospheric spots, faculae, and/or plages, are investigated. No correlation with Ca II H+K chromospheric activity indicators is observed. Multi-component LTE “toy” models have been constructed in order to simulate photospheric temperature inhomogeneities that could arise from the presence of starspots, and we demonstrate that photospheric spots are a plausible source of the triplet trends among the cool dwarfs.

Subject headings: open clusters and associations: individual(Hyades) — stars: abundances — stars: atmospheres — stars: late-type — stars: spots

1. INTRODUCTION

The derivation of stellar O abundances using spectra at visible wavelengths is generally limited to a small number of atomic features. The two sets of features most often used for O abundance determinations are a) two forbidden [O I] spectral lines at 6300.3 and 6363.8 Å, and b) the permitted high-excitation O I triplet in the 7771-7775 Å region. The formation of the [O I] lines is well described by current local thermodynamic equilibrium (LTE) calculations (Takeda 2003), but the lines are weak in the spectra of solar-type stars and suffer from blends (e.g., Johansson et al. 2003). High-quality spectra and knowledge of

the blending features are required if the forbidden lines are to be used for accurate abundance derivations. On the other hand, each line of the O I triplet is strong in the spectra of solar-type dwarfs and evolved stars at all metallicities, and they are presumably free from blends, making them a more attractive choice for O abundance studies. However, the O I triplet (henceforth the triplet) is known to be sensitive to non-LTE (NLTE) effects (Kiselman 1991), and there is much controversy regarding its delivery of accurate O abundances.

The formation of the triplet is due to a high-excitation electronic transition (9.15 eV above the ground state) from the 3s orbital into the 3p orbital, with the multiple lines of the feature resulting from three possible values of the total angular momentum (J) in the terminal state. The NLTE behavior of the triplet is due to the dilution of each line’s source function (S_l) compared to the Planck function in the line forming region (Kiselman 2001). Thus, O abundances derived using LTE calculations, which utilize a Planckian source function, are overestimated. The magnitude of the effect is expected to increase as the number of O atoms in the 3s state increases, for instance by an increase in the total number of O atoms, by a decrease in gas pressure, or by an increase in temperature in the line forming region (e.g., Takeda 2003, Kiselman 2001). In particular, Takeda (2003) has constructed an extensive collection of NLTE corrections for late-F through early-K stars in various evolutionary states with the general result that the NLTE corrections for a given adopted O abundance increase with increasing T_{eff} for all evolutionary states, with negligible corrections required for dwarfs with $T_{\text{eff}} < 6000$ K.

On the observational side, quantifying the NLTE behavior of derived triplet abundances is difficult because of the inhomogeneity of O abundances among field stars; star-to-star comparisons are generally not meaningful. This can be overcome by deriving simultaneously O abundances from the triplet and a feature predicted to be free from NLTE effects, such as $\lambda 6300$ [O I] line. For example, King & Boesgaard (1995) compared LTE O abundances as derived from the triplet and the $\lambda 6300$ [O I] in a sample of field dwarfs with a moderate range in metallicities ($-0.84 \leq [\text{Fe}/\text{H}] \leq +0.24$; $[\text{Fe}/\text{H}]$ is used throughout this paper as a fiducial for metallicity). No significant difference in the O abundance from the two indicators was found for stars with $T_{\text{eff}} \lesssim 6200$ K, but an increasing difference- presumably due to larger triplet abundances- with increasing T_{eff} was evident in the warmer stars of the sample. The results of the King & Boesgaard study are in good agreement with NLTE predictions. Many other studies have derived NLTE O abundances using the triplet, with varying results. Additional observational behavior of the triplet compared to other O spectral lines has been covered extensively in the literature (e.g., Fulbright & Johnson 2003; Nissen et al. 2002; Mishenina et al. 2000; Israelian, García López, & Rebolo 1998), and we point the reader interested in a more thorough discussion to those publications.

Another tactic to investigate triplet departures from LTE is to analyze O abundances of open cluster stars. Open clusters are stellar aggregates composed of members believed to have a common age and chemical composition. These shared characteristics make *intracluster* comparisons ideal for probing mass-dependent stellar effects and *intercluster* comparisons ideal for probing age-related or metallicity effects-. Surprisingly, only a handful of cluster O studies have been done. García López et al. (1993) subjected the triplet in spectra of 25 Hyades (600 Myr, $[\text{Fe}/\text{H}] = +0.13$) F dwarfs ($6045 \leq T_{\text{eff}} \leq 7375$ K), as well as 18 F dwarfs ($5850 \leq T_{\text{eff}} \leq 7110$ K) in the Ursa Major (UMa) kinematic moving group (600 Myr, $[\text{Fe}/\text{H}] = -0.09$), to an NLTE analysis. While good star-to-star agreement (within uncertainties) of the O abundances for both stellar samples was found, T_{eff} -dependent differences are seen when the stars are placed into T_{eff} bins. The mean bin O abundance decreases with decreasing T_{eff} for both the Hyades and UMa, raising questions as to the accuracy of the adopted NLTE corrections. King (1993) analyzed the triplet in the spectra of four Hyades dwarfs ($5772 \leq T_{\text{eff}} \leq 6103$ K) and found star-to-star agreement in the LTE O abundances. King et al. (2000) derived LTE O abundances from the triplet in two Pleiades (100 Myr, $[\text{Fe}/\text{H}] = 0.00$) and one NGC 2264 (10 Myr, $[\text{Fe}/\text{H}] = -0.15$) K-dwarfs. Given the relatively low T_{eff} for these stars ($4410 \leq T_{\text{eff}} \leq 4660$ K), NLTE effects on the formation of the triplet are predicted to be negligible (Takeda 2003), yet unexpectedly high O abundances were found for all three stars. No explanation for the high abundances was immediately obvious, but the authors speculated that yet unknown NLTE effects resulting from the presence of a chromosphere may be the cause (as suggested by Takeda 1995).

A more comprehensive study of LTE O abundances derived using the triplet in Pleiades dwarfs, as well as in M34 (200 Myr, $[\text{Fe}/\text{H}] = +0.07$) dwarfs, has been presented by Schuler et al. (2004; henceforth SKHP). The stellar sample includes 15 Pleiads with $5048 \leq T_{\text{eff}} \leq 6172$ K and eight M34 dwarfs with $5385 \leq T_{\text{eff}} \leq 6130$ K, and in both cases, a dramatic increase in triplet $[\text{O}/\text{H}]$ abundances with *decreasing* T_{eff} is seen for $T_{\text{eff}} \lesssim 5600$ K. The Pleiades results confirmed the high triplet-based O abundances initially reported by King et al. (2000) and are in contrast with canonical NLTE predictions. Furthermore, the Pleiades abundances evince scatter that exceeds uncertainties at $T_{\text{eff}} < 5300$ K. Following Takeda (1995), the triplet results were compared to $H\alpha$ and Ca II triplet chromospheric activity indicators from the literature. No correlations between O abundances and activity or O abundance scatter and activity scatter were found; it should be noted, however, that the O abundances and activity indices were not measured contemporaneously. SKHP proposed temperature inhomogeneities resulting from photospheric spots, faculae, and/or plagues (henceforth collectively referred to as spots) as a possible explanation for the high O abundances, being influenced by the work of Stauffer et al. (2003) who suggested the anomalously blue color excess of Pleiades K-dwarfs may be due to the presence of spots. King & Schuler

(2005) extended the study of the triplet to six UMa dwarfs in the T_{eff} range of 4925-5827 K, and the LTE O abundances show a similar increase with decreasing T_{eff} as seen in the Pleiades. The UMa trend, however, is shallower. The age and metallicity differences between the Pleiades and UMa suggest that triplet abundance trends observed among cool open cluster dwarfs might be influenced by effects related to either of these parameters.

The Hyades open cluster is the next logical target for our continued investigation of the ubiquity and nature of triplet-derived O abundance trends in cool cluster dwarfs. The cluster is observationally appealing because of the relative brightness of its members; late-K dwarfs are brighter than $V \sim 10.5$ and thus within the capabilities of moderate-sized telescopes. More importantly, the physical characteristics are well-suited for this study. Its members are metal-rich compared to those in both the Pleiades and UMa, and they have an age that is approximately coeval to UMa members (King & Schuler 2005). If a Hyades triplet trend is present, comparing its morphology to that of the Pleiades and UMa should provide valuable insight into its possible cause and evolution. Therefore, an LTE analysis of the triplet in high-resolution, high signal-to-noise (S/N) spectra obtained with the Mayall 4-m telescope and echelle spectrograph at Kitt Peak National Observatory and with the Harlan J. Smith 2.7-m telescope and the cross-dispersed echelle spectrometer at McDonald Observatory of 45 Hyades dwarfs is presented. The cool dwarf O abundances derived from the triplet are compared to previous open cluster results, and a plausible explanation for observed triplet trends is proffered.

2. OBSERVATIONS AND DATA REDUCTION

Hyades membership is well determined (Perryman et al. 1998), and the cluster is rich with G and K dwarfs. We made use of the recent studies of Yong et al. (2004) and Paulson et al. (2003) in constructing our target list, which contains 45 stars. The analysis presented herein makes use of three sets of high-resolution echelle spectra obtained with two telescopes on different dates. The majority of the sample were observed 2002 November 22-25 with the KPNO Mayall 4-m and accompanying Cassegrain echelle spectrograph. This sample will henceforth be referred to as KPNO-02. The $31.6 - 63 \text{ g mm}^{-1}$ echelle grating and $226 - 1 \text{ g mm}^{-1}$ cross disperser were used, resulting in a dispersion of $\sim 0.091 \text{ \AA pixel}^{-1}$ and a resolution $R = \lambda/\Delta\lambda \approx 43,000$ (~ 2.0 pixels) at 7775 \AA . The detector (T2KB) consists of $24 \text{ }\mu\text{m}$ pixels and has dimensions of 2048×2048 ; no binning was used.

The second set of spectra was also obtained with the KPNO Mayall 4-m telescope and echelle spectrograph; the observations took place on the dates of 2004 December 20-23 (henceforth KPNO-04). These later observations utilized the $58.5 - 63 \text{ g mm}^{-1}$ echelle

grating and the $226 - 1 \text{ g mm}^{-1}$ cross disperser. The data are characterized by a dispersion of $\sim 0.093 \text{ \AA pixel}^{-1}$ and a similar resolution of $R \approx 42,000$ (~ 2.0 pixels) at 7775 \AA . The T2KB detector was again used without binning.

The final set of spectra was obtained on 2004 October 10-12 with the Harlan J. Smith 2.7-m telescope and the "2dcoude" cross-dispersed echelle spectrometer at McDonald Observatory (henceforth McD-04). The cs23 setting and E2 echelle grating (52.7 g mm^{-1}) were used, giving a resolving power of $R \approx 60,000$ (~ 2.1 pixels) and dispersion of $\sim 0.063 \text{ \AA pixel}^{-1}$ at 7775 \AA . The angle of the echelle grating and cross dispersion prism was set manually so that the O I triplet fell well away from the edge of the detector. The TK3 detector, with $24 \mu\text{m}$ pixels, is a 2048×2048 square ccd, and it was used without binning. We note that one star (HIP 20146) was kindly acquired by Dr. J. Laird with the McDonald 2.7-m telescope in 1995 with a similar set-up as the 2004 2.7-m observations and is included in our sample. Its spectrum is of equal quality to the other McDonald data.

The stars in the combined sample are listed according to Hipparcos number, along with the HD number when available, in Table 1. The adopted stellar parameters (see below), as well as the telescope used to observe each object, are also presented therein. It will be noticed that a handful of stars have been observed during two different runs. This is beneficial in that it allows for the revelation of possible systematic errors that might be associated with a particular data set. A solar proxy spectrum of the daytime sky was obtained during each observing run, as is indicated in Table 1. The KPNO and McDonald data were reduced in a consistent fashion using IRAF³, following standard procedures of bias subtraction, flat fielding, correction for scattered light, extraction, and wavelength calibration. A sample spectrum from each data set is shown in Figure 1.

Tab. 1
Fig. 1

3. ANALYSIS AND RESULTS

3.1. Stellar Parameters

Effective temperatures have been derived photometrically following the procedure of Thorburn et al. (1993). Briefly, $(B - V)_0$ colors are transformed to $(V - K)_0$ colors using an empirical relation for Hyades dwarfs (Carney 1983). Effective temperatures are then derived using the $(V - K)$ - T_{eff} relation of Carney (1983) modified to include the zero-point

³IRAF is distributed by the National Optical Astronomy Observatories, which are operated by the Association of Universities for Research in Astronomy, Inc., under cooperative agreement with the National Science Foundation.

correction of Cayrel et al. (1985). The 1σ error in the resulting temperatures as reported by Thorburn et al. (1993) is ± 55 K. The $(B - V)$ colors for the largest number of stars are from Allende Prieto & Lambert (1999), and for the stars not appearing therein, the colors are from Paulson et al. (2003) or Yong et al. (2004).

Surface gravities ($\log g$) have been determined by making use of the latest Y² isochrones (Yi et al. 2003) and the interpolation routine provided by the Y² consortium⁴ to generate a stellar track suitable for the Hyades. The required cluster parameters for the interpolation are age, $[\text{Fe}/\text{H}]$, and α -enrichment ($[\alpha/\text{Fe}]$). There have been multiple studies on the age and Fe content of the Hyades. We have chosen an age of 600 Myr (e.g., Perryman et al. 1998; Torres, Stefanik, & Latham 1997) and a relative Fe abundance of $[\text{Fe}/\text{H}] = +0.13$ (Paulson et al. 2003). Paulson et al. also derived the abundances of the α elements Mg, Si, Ca, and Ti and found them to scale with Fe; thus the Hyades α -enrichment has been taken to be zero. Surface gravities and effective temperatures taken from the stellar track characterized by the above parameters were fit with a fourth order Legendre polynomial using the `curfit` utility within `IRAF`. This utility provides equivalent power series coefficients which were used to create a T_{eff} -dependent relation for $\log g$. The final $\log g$ values were calculated using the adopted T_{eff} described above. Additionally, the effect of the adopted stellar track parameters on the derived surface gravities has been tested by creating several additional stellar tracks interpolated with a mixture of relative iron abundances and ages ranging from $0.10 \leq [\text{Fe}/\text{H}] \leq 0.16$ and 600-700 Myr. The surface gravities derived from these different tracks never differ from the adopted values by more than 0.01 dex, demonstrating the insensitivity of the $\log g$ values for these main sequence (MS) dwarfs to the reasonable choice of cluster parameters. We have chosen a conservative 1σ error in $\log g$ of 0.10 dex.

Microturbulent velocities (ξ) are calculated using the empirical formula of Allende Prieto et al. (2004). The function predicts ξ values with an rms scatter of 0.14 km s^{-1} . We have chosen a 1σ uncertainty of 0.15 km s^{-1} in our ξ values. The adopted stellar parameters are given in Table 1.

3.2. Equivalent Widths

Continuum normalization and equivalent width (EW) measurements were carried out using the one-dimensional spectrum analysis package `SPECTRE` (Fitzpatrick & Sneden 1987). The triplet falls in two separate orders of the KPNO-02 data due to order overlap in the individual spectra. EWs of the triplet have been measured in both orders- designated as blue

⁴See <http://www.astro.yale.edu/demarque/yyiso.html>

and red- and abundances are derived using the blue, red, and mean EWs. Gaussian profiles were used to determine the EWs of the triplet feature; the three lines were measurable in the spectra of all the stars except for eight: two lines were measurable for seven stars and one line for one star. These eight stars are generally the coolest stars in the sample as the triplet feature becomes increasingly weak in the spectra of dwarfs with decreasing temperature, *ceteris paribus*. The dependence of triplet EWs on T_{eff} is clearly seen in Figure 2. Only stars for which all three lines were measurable are plotted in the figure, and thus all the stars cooler than ~ 4800 K are not included. Also apparent in Figure 2 is the uniformity of EW measurements at a given T_{eff} shared among the different data sets. This is encouraging and suggests our individual samples do not suffer from observation-dependent systematic errors. The measured EWs and the per pixel signal-to-noise (S/N) ratio, as given by Poisson statistics, in the $\lambda 7775$ region are given in Tables 2 and 3. Some of the stars were observed multiple times during a given run, and the EW and S/N measurements for these were made using the co-added spectra.

Fig. 2
Tab. 2

Empirical estimation of line strength uncertainties has been made by comparing the EWs from the blue and red orders of the KPNO-02 data. Line-by-line differences were calculated for each star in the KPNO-02 sample, and the mean difference for each line has been adopted as the 1σ uncertainty in the EW of the line. The final uncertainties are $4.4 \text{ m}\text{\AA}$ for $\lambda 7771.94$, $4.8 \text{ m}\text{\AA}$ for $\lambda 7774.17$, and $2.7 \text{ m}\text{\AA}$ for $\lambda 7775.39$ and have been adopted for the entire stellar sample. It should be noted that 35 out of 36 stars comprising the KPNO-02 data set have effective temperatures greater than 4800 K and thus have larger EWs than the cooler stars in the sample. The adopted line strength uncertainties represent a far larger percentage of the EWs of the weaker features in the coolest stars and may not accurately reflect the errors associated with their measurement. Indeed, comparing the line strengths from the blue and red orders of the coolest star in the KPNO-02 sample (HIP 18322) gives uncertainties of 0.4 and $0.7 \text{ m}\text{\AA}$ for the $\lambda 7774.17$ and $\lambda 7775.39$ lines, respectively; the $\lambda 7771.94$ line was not measurable for this star. Nonetheless, we conservatively adopt the larger EW uncertainties for the whole stellar sample. The final uncertainties in the derived abundances for the coolest stars are clearly dominated by the line strength errors and are large relative to the warmer stars; however, the final conclusions of this work remain unchanged.

3.3. Oxygen Abundances

Oxygen abundances have been derived following the procedure of SKHP using an updated version of the LTE stellar line analysis software package MOOG (Snedden 2004, private communication). Atomic data ($\chi_{7772} = \chi_{7774} = \chi_{7775} = 9.15 \text{ eV}$; $\log gf_{7772} =$

0.369, $\log gf_{7774} = 0.223$, and $\log gf_{7775} = 0.001$) are from the NIST⁵ database. Stellar atmosphere models characterized by the adopted stellar parameters and $[\text{Fe}/\text{H}] = +0.13$ (Paulson et al. 2003) were interpolated from the ATLAS9 (LTE) grids of R. Kurucz⁶. The grids utilized here include the convective overshoot approximation. The validity of using the overshoot models of Kurucz to derive Fe abundances for Hyades dwarfs has recently been questioned (Paulson et al. 2003), who suggest Kurucz grids without convective overshoot are more appropriate. However, SKHP derived triplet abundances in Pleiades and M34 dwarfs utilizing four different sets of ATLAS9 grids, including Kurucz grids with and without overshoot, and found the results to be independent of model atmosphere. Models with convective overshoot have been used here due to the availability of finer super-solar metallicity steps for these grids compared to grids without the overshoot approximation.

The derived mean O abundances and final internal uncertainties are presented in Table 4; the abundances are given relative to solar values (using the usual notation $[\text{O}/\text{H}] = \log N(\text{O})_{\text{Star}} - \log N(\text{O})_{\odot}$ on a scale where $\log N(\text{H}) = 12.0$) via a line-by-line comparison. Solar abundances were derived in the same manner as the rest of the sample from spectra obtained during each observing run; each solar spectrum was used for comparison with only those stars observed during the same observing run. Abundance sensitivities to the adopted stellar parameters were determined by constructing additional model atmospheres characterized by single parameter changes of ± 150 K in T_{eff} , ± 0.25 dex in $\log g$, and ± 0.30 km s⁻¹ in ξ for each star and deriving the adjusted abundances in the same manner as above; typical sensitivities are given in Table 5. The resulting parameter-dependent abundance uncertainties are summed quadratically with uncertainties in line strengths and in the mean abundances to achieve the final internal uncertainties.

Tab. 3
Tab. 4

In Figure 3 the relative O abundances and associated error bars, as well as the line-by-line relative abundances for each star, are plotted against T_{eff} . The KPNO-02 abundances are those derived using the mean EWs. The error bars for the coolest stars are significantly larger than those for the warmer stars due to the large adopted EW uncertainties relative to the cool object line strengths, as described above. Regardless, a smooth increase in $[\text{O}/\text{H}]$ vs T_{eff} is clearly seen for stars with $T_{\text{eff}} < 5500$ K, as well as an apparent increase for stars with $T_{\text{eff}} > 6200$ K. Also apparent is the lack of star-to-star scatter in the $[\text{O}/\text{H}]$ abundances, in contrast to that observed among cool Pleiades dwarfs (SKHP). Abundances for stars that are common to more than one data set are given in Table 6. Comparing results from the different data sets reveals no statistically significant deviations. This was suggested by the

⁵<http://physics.nist.gov/PhysRefData/ASD/index.html>

⁶See <http://kurucz.harvard.edu/grids.html>

uniformity of EWs in Figure 2, and more strongly demonstrated here. We are confident that no large systematic differences exist between the data sets, and they will no longer be distinguished.

There are also no systematic differences in the line-by-line O abundances (Figure 3), which are in good agreement for each star and provide strong evidence that the triplet is not hampered by blends. Possible exceptions are the two coolest stars, HIP 19441 and HIP 20762. Only two of the three lines of the triplet were measurable for these two stars, and in each case, the abundance of the $\lambda 7774$ line is ~ 0.20 dex larger than that of the other measurable line. There is an Fe I line at $\lambda = 7774.00 \text{ \AA}$ ($\chi = 5.01 \text{ eV}$) (Takeda et al. 1998) that may be enhancing the line strength of the $\lambda 7774$ O feature in the spectra of the coolest stars, and we have used MOOG to synthesize the triplet region of HIP 19441 in order to determine the magnitude of this effect. According to the relative line strength parameter provided by MOOG, the O line is expected to be an order of magnitude stronger than the Fe line, suggesting that this particular Fe feature is not responsible for the enhanced EW of the $\lambda 7774$ O line. Alternatively, systematic errors related to measuring the weak triplet in the spectra of the coolest dwarfs or a yet to be identified blend may be the cause of the seemingly higher abundance provided by the $\lambda 7774$ line. Regardless, if the abundance of the $\lambda 7774$ feature is ignored for the two coolest stars, the morphology of the cool dwarf abundance trend is not greatly affected.

One star, HIP 15310, has an O abundance that deviates from those of stars in the sample with similar T_{eff} ($\sim 5870 \text{ K}$). Paulson et al. (2003) reports a Fe abundance for HIP 15310 that is larger than the cluster mean and introduced the possibility that this star might have been chemically enriched, possibly by the accretion of proto-planetary or planetary material. The observational evidence that host stars of the discovered planetary systems are statistically more Fe-rich compared to otherwise similar field stars that do not have planets is now well established (Fischer & Valenti 2005). Two theories to explain the higher metallicity of planetary hosts have been discussed in the literature: a) planets form preferentially in high-metallicity environments, or b) planetary hosts are chemically enriched due to planetary accretion. Gonzalez (1997) suggested that a possible signature of accretion would be abundance enhancements correlated with condensation temperature. Oxygen is a volatile element with a condensation temperature of $\sim 180 \text{ K}$ (in a gas of solar composition), and Fe is a refractory element with a condensation temperature of $\sim 1340 \text{ K}$ (Lodders 2003). While a larger fraction of the initial O abundance of a gas condenses into rocky material than of other volatile elements- due to its role in the formation of silicates and oxides- the increase in its abundance in a stellar photosphere compared to refractory elements such as Fe should not be as significant if accretion has taken place. Adopting a mean Hyades O abundance using the stars in the T_{eff} range of 5450-6100 K (the T_{eff} range over which there

Fig. 3
Tab. 5

is good agreement in O abundances; see below) and the mean cluster Fe abundance from Paulson et al. (2003), a cluster $[\text{O}/\text{Fe}]$ ratio of +0.12 is attained. Paulson et al. derived an Fe abundance of $[\text{Fe}/\text{H}] = +0.30$ for HIP 15310, and comparing this to the O abundance found here, $[\text{O}/\text{Fe}] = +0.08$ for this star. From these results, it is apparent that HIP 15310 has not been chemically enriched by fractionated material, although more quantitative data on the expected relative O and Fe enhancements due to accretion are in order. Based on previous membership studies, Paulson et al. (2003) also question the cluster membership of HIP1 15310. Further investigation of HIP 15310 and its possible chemical enrichment is beyond the scope of this paper but certainly should be addressed in future studies.

4. DISCUSSION

Although the $[\text{O}/\text{H}]$ abundances of the warmest stars ($T_{\text{eff}} > 6150$ K) in the sample agree with those of slightly cooler stars within the calculated uncertainties (Figure 3), the abundances appear to be increasing with increasing T_{eff} . This behavior is consistent with previous triplet LTE abundance derivations of near-solar metallicity dwarfs (King & Boesgaard 1995) and with expectations from canonical NLTE calculations (e.g., Takeda 2003). More interesting is the trend of increasing $[\text{O}/\text{H}]$ abundances with *decreasing* T_{eff} , which is not congruous with expectations for open cluster stars nor predicted by NLTE calculations. In fact, NLTE corrections for MS dwarfs with $T_{\text{eff}} \lesssim 5500$ K are predicted to be less than 0.05 dex and *decrease* with *decreasing* T_{eff} according to Takeda (2003).

The triplet is highly sensitive to T_{eff} , and thus the cool dwarf O abundance trend may be a consequence of the adopted T_{eff} scale. At ~ 45 pc, the Hyades is the nearest open cluster and is well-studied photometrically and astrometrically, making the use of a color-temperature relation a seemingly reasonable choice for derivations of Hyades dwarf T_{eff} . However, Pinsonneault et al. (2004) was unable to fit an isochrone to the photometry of the Hyades cluster, especially for the reddest stars, using several color-temperature relations from the literature. They go on to demonstrate that their empirically calibrated luminosity-based temperature scale is in better agreement with the spectroscopically derived temperatures of Paulson et al. (2003) and argue the mismatch between photometry and theoretical colors is due to systematic errors in the color-temperature relations. In order to test the sensitivity of the cool dwarf abundances to our adopted photometric T_{eff} scale, temperatures using the empirically calibrated Hyades isochrone of Pinsonneault et al. (2004; T_{PTHs}) and the metallicity-dependent temperature-color calibration of Ramírez & Meléndez (2005; T_{IRFM}) have been derived. The temperature scale of Ramírez & Meléndez is derived using the infrared flux method (IRFM; Blackwell et al. 1990) and is an extension of the work of

Alonso, Arribas, & Martínez-Roger (1996, 1999). The B-V colors from Table 1 and a cluster metallicity of $[\text{Fe}/\text{H}] = 0.13$ were used to derive T_{IRFM} from the calibration of Ramírez & Meléndez (we use the coefficients for the metallicity-dependent polynomial correction that are applicable for $-0.5 < [\text{Fe}/\text{H}] < +0.5$).

In Figure 4a, T_{PTHS} and T_{IRFM} are plotted against the adopted photometric T_{eff} . The Pinsonneault et al. isochrone-based temperatures of all but seven stars are higher than our adopted ones; temperature differences on a star-by-star basis are $|T_{\text{PTHS}} - T_{\text{eff}}| \leq 152$ K, with differences for about half of the sample being < 60 K. Temperatures from the temperature-color calibration of Ramírez & Meléndez are in better agreement with T_{eff} , with star-by-star differences being $|T_{\text{IRFM}} - T_{\text{eff}}| \leq 57$ K, with all but nine having differences ≤ 30 K. For both T_{PTHS} and T_{IRFM} , absolute differences with T_{eff} are approximately less than or equal to the 1σ error T_{eff} , and thus no large-scale differences are found. Oxygen abundances have been rederived using the new temperatures, and the results are plotted along with the original values in Figure 4b. The abundances in Figure 4b have been culled of duplicates; in cases of overlap, preferred abundances are taken from the data set following the order KPNO-02, KPNO-04, and McD-04. The KPNO-02 abundances are those derived using the mean EWs, as described above. In the intermediate T_{eff} range of 5450-6100 K, the abundances of the dwarfs derived using T_{PTHS} are on average 0.06 dex lower than the original abundances. Outside of this intermediate T_{eff} range, the trends of increasing O abundances among both the warm and cool dwarfs remain. The abundances derived using T_{IRFM} do not differ significantly from the original abundances, and again, the cool dwarf abundance trend persists. In both cases, the differences in the abundances of the coolest stars are of the greatest magnitude, but they are generally within the calculated uncertainties. *The pertinent result of this exercise is that the triplet abundance trend among the cool Hyades dwarfs presented here is apparently not due to an inaccurate T_{eff} scale.* A similar conclusion was reached by SKHP in their study of the triplet in Pleiades dwarfs. This result is not surprising given the abundance sensitivities in Table 5. For the coolest stars in the sample, a T_{eff} change of over 400 K would be required to bring their abundances into concordance with those of the intermediate T_{eff} stars, where there is good star-to-star agreement. Comparing the adopted photometric T_{eff} scale to those of Pinsonneault et al. and of Ramírez & Meléndez suggests that uncertainties in our temperatures may be as high as 150 K, which is significantly less than what is required to eliminate the cool dwarf abundance trend.

Fig. 4

The morphology of the Hyades cool dwarf ($T_{\text{eff}} \leq 5450$ K) abundances is qualitatively similar to that recently seen in Pleiades dwarfs (SKHP), but significant differences do exist. The Hyades $[\text{O}/\text{H}]$ abundances sans duplicates and the SKHP Pleiades $[\text{O}/\text{H}]$ abundances (derived using Kurucz models with no convective overshoot) are plotted in Figure 5. The typical uncertainty in the Pleiades abundances is ± 0.08 dex. Although there are more

Hyades stars with $T_{\text{eff}} > 5200$ K, no difference in the triplet abundances of the two clusters in this T_{eff} region is discernible. This in itself is striking given that Hyades stars are metal-rich compared to Pleiades ($[\text{Fe}/\text{H}] \approx 0.00$; Boesgaard & Friel 1990) stars, suggesting the Pleiades $[\text{O}/\text{Fe}]$ ratio could be as much as 0.13 dex higher than the Hyades. It has been demonstrated that even a moderate, non-zero $[\text{O}/\text{Fe}]$ ratio can have a significant effect on pre-main sequence (PMS) Li depletion predictions (Swenson et al. 1994; Piau & Turck-Chièze 2002), and because of the prominent roles the Pleiades and Hyades play in the study of Li depletion mechanisms (e.g., Ford, Jeffries, & Smalley 2002), the potentially larger $[\text{O}/\text{Fe}]$ ratio for the Pleiades relative to the Hyades must be taken into consideration.

Fig. 5

For stars with $T_{\text{eff}} < 5200$ K, the $[\text{O}/\text{H}]$ abundances of the two clusters clearly diverge, with the Hyades trend being less steep than that for the Pleiades. The Hyades $[\text{O}/\text{H}]$ abundances were fit with a quadratic function, and the reduced χ^2 between this fit and the Pleiades data was calculated. Based on this, the Pleiades abundances deviate from those of the Hyades at a confidence level of $> 99.999\%$. In an attempt to explain this divergence and, as a result, shed light on the nature of the increasing triplet abundances with decreasing T_{eff} , one naturally turns to the two possibly relevant physical characteristics that are disparate between these two clusters: metallicity and age. A similar suggestion is offered by King & Schuler (2005) who compared their triplet results of six UMa dwarfs to the SKHP Pleiades abundances and found the UMa trend to be shallower than the Pleiades. The UMa moving group is characterized by a sub-solar Fe abundance of $[\text{Fe}/\text{H}] = -0.09$ (Boesgaard & Friel 1990) and an age that is approximately coeval to the Hyades (King & Schuler 2005); UMa is an excellent sample with respect to the Hyades and Pleiades results to perform an empirical test of the sensitivity of the $[\text{O}/\text{H}]$ trends to metallicity and age. Accordingly, the King & Schuler $[\text{O}/\text{H}]$ UMa abundances are included in Figure 5. In order to put the UMa abundances on a scale similar to the Hyades and Pleiades, the abundances have been increased by a constant to bring the abundance of the warmest UMa star into concordance with the mean abundance for Hyads in the range of $5450 \leq T_{\text{eff}} \leq 6000$ K, the temperature range in which the two warmest UMa stars are located. If metallicity is a factor, then an UMa trend that is steeper than the Pleiades trend would be expected. Despite the paucity of UMa data points, this is clearly not seen. Indeed, for stars with $T_{\text{eff}} \leq 5300$ K, the UMa abundances map well with the Hyades trend. These limited data, while not conclusive, instead point to an age-related effect influencing the triplet abundance trends in cool cluster dwarfs. We now turn our attention to two age-related phenomena previously suggested to possibly affect triplet abundances: chromospheric activity and photospheric spots.

4.1. Chromospheric Activity

The effects of a global chromosphere on the formation of spectral lines are not well understood. There is some evidence that the large spread in Li abundances among Pleiades K-dwarfs is correlated with chromospheric activity indicators (King & Schuler 2004; Soderblom et al. 1993), but it is far from clear whether the correlation is causal. With respect to O, Takeda (1995) found appreciable increases in the modeled line strengths of the triplet in the solar spectrum when using Kurucz atmospheres modified to include a chromosphere. The increase is apparently due to the temperature rise at depths $\tau_{5000} \lesssim 10^{-4}$ and to the large fraction of O atoms that remain neutral. SKHP compared the O abundances derived from the triplet for the Pleiades and M34 to $H\alpha$ and Ca II triplet chromospheric activity measures from the literature and found no correlation. A similar analysis for the Hyades sample is presented in Figure 6, where our [O/H] abundances are plotted against Ca II H+K activity indicators (Paulson et al. 2002) and against differences in observed and T_{eff} -dependent mean values ($\Delta R'_{\text{HK}}$). No statistically significant correlation exists for either comparison. Thus, the combined Hyades and Pleiades results suggest a global chromosphere does not contribute to triplet trends among cool cluster dwarfs.

Fig. 6

More recently, Morel & Micela (2004) analyzed the triplet and [O I] $\lambda 6300$ forbidden line in spectra of 14 single-lined, chromospherically active RS CVn binaries, and in Pleiades, Hyades, and field dwarf, as well as in field giant, data from the literature. They report increasingly discrepant results between the two indicators with higher chromospheric activity levels, with the discrepancy primarily due to increasing triplet abundances (see Figure 1 therein). In general, the inconsonant results are restricted to the RS CVn binaries and the Pleiades dwarfs- the other stellar subsets generally have lower levels of chromospheric activity and do not evince a triplet-activity correlation. With regards to the Pleiades dwarfs (the [O/H] and color-based T_{eff} data for which are taken from SKHP), a correlation between triplet [O/Fe] abundances and X-ray-based activity indicators (R_X - ratio of X-ray and bolometric luminosities) at a confidence level of $> 98\%$ is reported. This should be viewed with caution due to the correlation (at the $\sim 97\%$ confidence level according to the linear correlation coefficient; data taken from Table 2 of Morel & Micela 2004) between the Pleiades R_X and T_{eff} , and to the fact that the [O/Fe] abundances are highly correlated with T_{eff} ($> 99.9\%$). The degeneracy of these correlations prevents firm conclusions from being made, and it is possible that the [O/Fe]- R_X activity relation might be due to other T_{eff} -related effects. Indeed, Morel & Micela state the Pleiades [O/H]- T_{eff} relation found by SKHP may be masking an activity effect given the tight correlation between $(B - V)_0$ - R_X as reported by Micela et al. (1999); however, the converse argument is equally valid, i.e., the [O/Fe]-activity relation is masking a T_{eff} effect. Because no correlation between Pleiades triplet [O/H] abundances and $H\alpha$ and Ca II chromospheric activity indicators exists, we find the

data supporting a triplet-activity relation for the Pleiades unconvincing.

For the RS CVn binaries, the interpretation of the Morel & Micela results and their relevance to the current study are not clear. The triplet [O/Fe] abundances of the Rs CVn stellar subset show a statistically significant correlation at the $\sim 96\%$ confidence level with Ca II H+K activity indicators, but a correlation with R_X indicators is totally absent. On the other hand, both activity indicators are not correlated with T_{eff} , but the [O/Fe] abundances are correlated with T_{eff} at a $> 99.9\%$ confidence level. These relations do not provide a definitive picture of the connection between activity and the triplet O abundances for these stars, especially when the nature and inhomogeneity of the sample are considered. RS CVn systems have enhanced chromospheric and photospheric (spots) activity, presumably due to effects resulting from interactions between the binary components. The primary components are generally evolved stars, and the Morel & Micela sample is composed mostly of sub-giants, according to the derived surface gravities (Morel et al. 2003; Morel et al. 2004). Thus, comparing the RS CVn triplet results to those of the Hyades and Pleiades dwarfs may be unwarranted.

4.2. Photospheric Spots

The effect of photospheric spots on abundance derivations has received a healthy amount of attention in the literature, especially with respect to Li abundances as measured from the $\lambda 6707$ resonance feature (e.g., Xiong & Deng 2005; Ford et al. 2002). Unfortunately, such analyses are limited to speculation because spots and their areal coverage of stellar surfaces are not well understood. The advent of doppler imaging has permitted the mapping of stellar surfaces and confirmed the presence of spots on target stars, but the technique is limited to stars with high rotational velocities ($40 \leq v \sin i \leq 80 \text{ km s}^{-1}$; Vogt & Penrod 1983). In order to reduce the rotationally-induced broadening of spectral features, stars that are typically included in abundance analyses are slow rotators and thus are not suitable for doppler imaging studies.

Nonetheless, we have undertaken a plausibility study to investigate whether the presence of spots could produce the anomalous triplet O abundances observed among our cool Hyades dwarf sample. We have utilized “toy” model atmospheres that include flux contributions to the triplet region from both cool and hot spots, as well as from the quiescent star. Our modeling scheme is a gross oversimplification of a complex interplay of atmospheric physics (i.e., magnetic fields, etc.) and temperature inhomogeneities, but it is useful as a first approximation of spot effects. The first criterion to which our multi-component toy models adhere is the conservation of total luminosity, similar to that described by Ford et al. (2002),

by using a weighted Stefan-Boltzmann relation:

$$T_{\text{eff}} = a_{\text{cool}}T_{\text{cool}}^4 + a_{\text{hot}}T_{\text{hot}}^4 + a_{\text{star}}T_{\text{star}}^4$$

where T_{eff} is the adopted effective temperature for the star (Table 1), a_{cool} , a_{hot} , and a_{star} are the areal coverages of the cool spots, hot spots, and quiescent star, respectively, and T_{cool} , T_{hot} , and T_{star} are the corresponding temperatures. The sum of the areal coverages are constrained such that

$$a_{\text{cool}} + a_{\text{hot}} + a_{\text{star}} = 1.$$

Areal coverages of $a_{\text{cool}} = a_{\text{hot}} = 0.20$ and initial spot temperatures were chosen arbitrarily, and the Stefan-Boltzmann relation was then solved for T_{star} . Three model atmospheres characterized by either T_{cool} , T_{hot} , or T_{star} were constructed; surface gravities and microturbulent velocities remain unchanged for the three models for each star and are as they appear in Table 1. With an input O abundance equal to the mean abundance of Hyads in the range of $5450 \leq T_{\text{eff}} \leq 6100$ K ($[\text{O}/\text{H}] = +0.25$), cool, hot, and star component spectra were synthesized using **MOOG**. Before combining the spectra into a composite spectrum, the contribution of flux at 7774 \AA - approximately at the center of the O I triplet- from the three temperature components was determined by solving the Planck function for each. The resulting values were then normalized to create a “Planck factor”. Each component spectrum was multiplied by its areal coverage and Planck factor, and finally the components were added to achieve a composite spectrum. The cool and hot temperatures were altered and the procedure iterated until the measured EWs of the composite spectrum were approximately equal (typically to within the measured EW uncertainties) to the observed EWs.

A sample of the component and composite spectra of HIP 18322 is presented in Figure 7, and the results of this exercise for three Hyads are given in Table 7. Assuming reasonable spot coverages and temperatures given in Table 7, the toy model employed here is able to satisfactorily reproduce the observed line strengths for all three stars. It is evident from Figure 7 that if spots affect observed triplet line strengths, the dominant contribution comes from hot spots, i.e., faculae and/or plagues; the cool spot regions have little or no effect. This provides significant freedom in choosing the spot coverages and temperatures for the present case, and it excludes uniqueness for our models. A more sophisticated approach to this problem could include other spectral features, including molecular lines, with differing T_{eff} sensitivities in order to constrain the areal coverages and temperatures of the models, assuming there are other features that show T_{eff} relations similar to the triplet. There are existing data suggesting this to be the case (e.g., SKHP). While this exercise is in no way conclusive, we have been able to demonstrate that photospheric temperature inhomogeneities can possibly account for the high triplet abundances of the cool Hyades dwarfs presented here and thus possibly produce the triplet abundance trends observed in cool open cluster

dwarfs.

Fig. 7
Tab. 6

5. SUMMARY AND CLOSING REMARKS

Oxygen abundances have been derived under the assumption of LTE from the high-excitation O I triplet in high-resolution spectra for 45 Hyades dwarfs in the effective temperature range of 4300–6300 K. The warmest stars in the sample ($T_{\text{eff}} > 6200$ K) show evidence of increasing triplet abundances with increasing T_{eff} , as predicted by current NLTE calculations. A striking increase of triplet abundances with *decreasing* T_{eff} is observed for stars with $T_{\text{eff}} < 5450$ K, contrary to expectations and to NLTE predictions. Triplet abundances have been rederived using two additional temperature scales, and the morphology of the cool dwarf abundance trend is unaltered, suggesting the trend is not due to erroneous T_{eff} . Comparing the Hyades trend to that previously observed among Pleiades dwarfs (SKHP) reveals both similarities and differences. At T_{eff} greater than ~ 5200 K, no difference in the abundances at a given T_{eff} for the two clusters is discernible, raising the possibility of a larger [O/Fe] ratio for the Pleiades relative to the Hyades. For stars with T_{eff} less than ~ 5200 K, the two trends diverge with the Hyades trend being less steep than that for the Pleiades. Another difference is the star-to-star abundance scatter seen for Pleiades with $T_{\text{eff}} < 5300$ K is not seen among the Hyades.

Recently derived triplet abundances for six dwarfs that are members of the Ursa Major moving group are compared to the Hyades and Pleiades results. UMa members have a sub-solar metallicity ([Fe/H] = -0.09 ; Boesgaard & Friel 1990), and an age that is approximately coeval with that of the Hyades (King & Schuler 2005). Despite the small number of UMa stars, their abundances closely follow the Hyades results, suggesting an age-related effect, as opposed to metallicity, is a material factor in triplet O abundance trends in cool cluster dwarfs. No correlation is found between Ca II H+K activity chromospheric activity indicators and Hyades [O/H] abundances. SKHP report a similar lack of correlation between $H\alpha$ and Ca II triplet chromospheric activity indicators and Pleiades triplet O abundances. Thus, we are unable to find evidence for an activity-triplet relation as suggested by the theoretical results of Takeda (1995). On the other hand, we demonstrate to first order that photospheric temperature inhomogeneities possibly due to spots, faculae, and/or plages can plausibly produce anomalously high triplet abundances. A simple toy model consisting of arbitrarily chosen line flux contributions from cool and hot spots is able to reproduce observed equivalent widths for three Hyads with differing T_{eff} and triplet abundances. The results do not conclusively point to spots as the source of the triplet trends in cool cluster dwarfs, but they are provocative and require further investigation.

There is concordance among the triplet O abundances for stars in the intermediate T_{eff} range of 5450-6100 K. Over this T_{eff} range, the NLTE corrections of Takeda (2003) differ by ≤ 0.05 dex, and thus the abundances given relative to solar values are essentially free of NLTE-related anomalies. The mean abundance for this group of 15 stars (excluding HIP 15310 which has questionable cluster membership) is $[\text{O}/\text{H}] = +0.25 \pm 0.02$, where the quoted error is the uncertainty in the mean. This value is in good agreement with that found by King (1993), who derived an LTE abundance using the triplet of $[\text{O}/\text{H}] = +0.22 \pm 0.04$ ⁷. García López et al. (1993) performed an NLTE analysis of the triplet in 25 Hyades F dwarfs and reported a mean O abundance of -0.06 ± 0.15 . This value is appreciably lower than that of the present study and of King (1993). The difference in the García López et al. and the King 1993 results is discussed thoroughly in King & Hiltgen (1996), who come to the conclusion that the bulk of the difference is most likely due to the NLTE corrections adopted by García López et al. and to different solar EWs adopted by the two studies. Finally, King & Hiltgen (1996) derived a Hyades O abundance from two dwarfs using spectral synthesis of the $\lambda 6300$ [O I] feature and find a mean abundance of $[\text{O}/\text{H}] = +0.15 \pm 0.01$. Comparing this result with that of the triplet in the intermediate group of stars here reveals a ~ 0.10 dex difference, possibly indicating the presence of underestimated internal errors or unaccounted for systematic errors in one or both studies. For instance, if the luminosity-based T_{eff} scale from the Hyades isochrone of Pinsonneault et al. (2004) is used to derive the triplet abundances of the intermediate group of stars, the mean abundance reduces to $[\text{O}/\text{H}] = +0.19 \pm 0.02$. If we take the [O I]-based and triplet-based O abundances as lower and upper limits, respectively, it appears the Hyades O abundance falls in the range of $0.15 \lesssim [\text{O}/\text{H}] \lesssim 0.25$ dex.

S.C.S. thanks the South Carolina Space Grant Consortium for providing support through the Graduate Student Research Fellowship. S.C.S. and J.R.K. gratefully acknowledge support for this work by grants AST 00-86576 and AST 02-39518 to J.R.K. from the National Science Foundation. D.M.T. and M.H.P. thank the National Science Foundation for support from grants AST-0205789 and AST-0206008 to the Ohio State University Research Foundation. We also thank Ms. Abigail Daane, Mr. Roggie Boone, and Ms. Angela Hansen for their assistance with the McD-04, KPNO-04, and KPNO-02 observations. This research has made use of the SIMBAD database, operated at CDS, Strasbourg, France and NASA’s Astrophysics Data System Bibliographic Services. We would like to acknowledge the anonymous referee, whose comments have led to an improved paper.

⁷The quoted abundance from King 1993 is that using an updated measurement of the EW for one of his program stars, as described by King & Hiltgen 1996

REFERENCES

- Allende Prieto, C., Barklem, P. S., Lambert, D. L., & Cunha, K. 2004, *A&A*, 420, 183
- Allende Prieto, C., & Lambert, D. L. 1999, *A&A*, 352, 555
- Alonso, A., Arribas, S., & Martínez-Roger, C. 1996, *A&AS*, 117, 227
- Alonso, A., Arribas, S., & Martínez-Roger, C. 1999, *A&AS*, 140, 261
- Blackwell, D. E., Petford, A. D., Arribas, S., Haddock, D. J., & Selby, M. J. 1990, *A&A*, 232, 396
- Boesgaard, A. M., & Friel, E. D. 1990, *ApJ*, 351, 467
- Carney, B.W. 1983, *AJ*, 88, 623
- Cayrel, R., Cayrel de Strobel, G., & Campbell, B. 1985, *A&A*, 146, 249
- Fischer, D. A., & Valenti, J. 2005, *ApJ*, 622, 1102
- Fitzpatrick, M. J., & Sneden, C. 1987, *BAAS*, 19, 1129
- Ford, A., Jeffries, R. D., & Smalley, B. 2002, *A&A*, 391, 253
- Fulbright, J. P., & Johnson, J. A. 2003, *ApJ*, 595, 1154
- García López, R. J., Rebolo, R., Herrero, A., & Beckman, J. E. 1993, *ApJ*, 412, 173
- Gonzalez, G. 1997, *MNRAS*, 285, 403
- Israelian, G., García López, R. J., & Rebolo, R. 1998, *ApJ*, 507, 805
- Johansson, S., Litzén, U., Lundberg, H., & Zhang, Z. 2003, *ApJ*, 584, L107
- King, J.R. 1993, Ph.D. dissertation, University of Hawaii
- King, J. R., & Boesgaard, A. M. 1995, *AJ*, 109, 383
- King, J. R., & Hiltgen, D. D. 1996, *AJ*, 112, 2650
- King, J. R., & Schuler, S. C. 2004, *AJ*, 128, 2898
- King, J. R., & Schuler, S. C. 2005, *PASP*, submitted
- King, J. R., Soderblom, D. R., Fischer, D., & Jones, B. F. 2000, *ApJ*, 533, 944

- Kiselman, D. 1991, *A&A*, 245, L9
- Kiselman, D. 2001, *New Astronomy Review*, 45, 559
- Lodders, K. 2003, *ApJ*, 591, 1220
- Micela, G., et al. 1999, *A&A*, 341, 751
- Mishenina, T. V., Korotin, S. A., Klochkova, V. G., & Panchuk, V. E. 2000, *A&A*, 353, 978
- Morel, T., & Micela, G. 2004, *A&A*, 423, 677
- Morel, T., Micela, G., Favata, F., Katz, D., & Pillitteri, I. 2003, *A&A*, 412, 495
- Morel, T., Micela, G., Favata, F., & Katz, D. 2004, *A&A*, 426, 1007
- Nissen, P. E., Primas, F., Asplund, M., & Lambert, D. L. 2002, *A&A*, 390, 235
- Paulson, D.B., Sneden, C., & Cochran, W.D. 2003, *AJ*, 125, 318
- Paulson, D. B., Saar, S. H., Cochran, W. D., & Hatzes, A. P. 2002, *AJ*, 124, 572
- Perryman, M. A. C., et al. 1998, *A&A*, 331, 81
- Piau, L., & Turck-Chièze, S. 2002, *ApJ*, 566, 419
- Pinsonneault, M. H., Terndrup, D. M., Hanson, R. B., & Stauffer, J. R. 2004, *ApJ*, 600, 946
- Ramírez, I., & Meléndez, J. 2005, *ApJ*, 626, 465
- Schuler, S. C., King, J. R., Hobbs, L. M., & Pinsonneault, M. H. 2004, *ApJ*, 602, L117 (SKHP)
- Soderblom, D. R., Jones, B. F., Balachandran, S., Stauffer, J. R., Duncan, D. K., Fedele, S. B., & Hudon, J. D. 1993, *AJ*, 106, 1059
- Stauffer, J. R., Jones, B. F., Backman, D., Hartmann, L. W., Barrado y Navascués, D., Pinsonneault, M. H., Terndrup, D. M., & Muench, A. A. 2003, *AJ*, 126, 833
- Swenson, F. J., Faulkner, J., Iglesias, C. A., Rogers, F. J., & Alexander, D. R. 1994, *ApJ*, 422, L79
- Takeda, Y. 1995, *PASJ*, 47, 463
- Takeda, Y., Kawanomoto, S., & Sadakane, K. 1998, *PASJ*, 50, 97

- Takeda, Y. 2003, *A&A*, 402, 343
- Thorburn, J. A., Hobbs, L. M., Deliyannis, C. P., & Pinsonneault, M. H. 1993, *ApJ*, 415, 150
- Torres, G., Stefanik, R. P., & Latham, D. W. 1997, *ApJ*, 474, 256
- Vogt, S. S., & Penrod, G. D. 1983, *PASP*, 95, 565
- Xiong, D.-R., & Deng, L. 2005, *ApJ*, 622, 620
- Yi, Sukyoung, Kim, Yong-Cheol, & Demarque, P. 2003, *ApJS*, 144, 259
- Yong, D., Lambert, D. L., Allende Prieto, C., & Paulson, D. B. 2004, *ApJ*, 603, 697

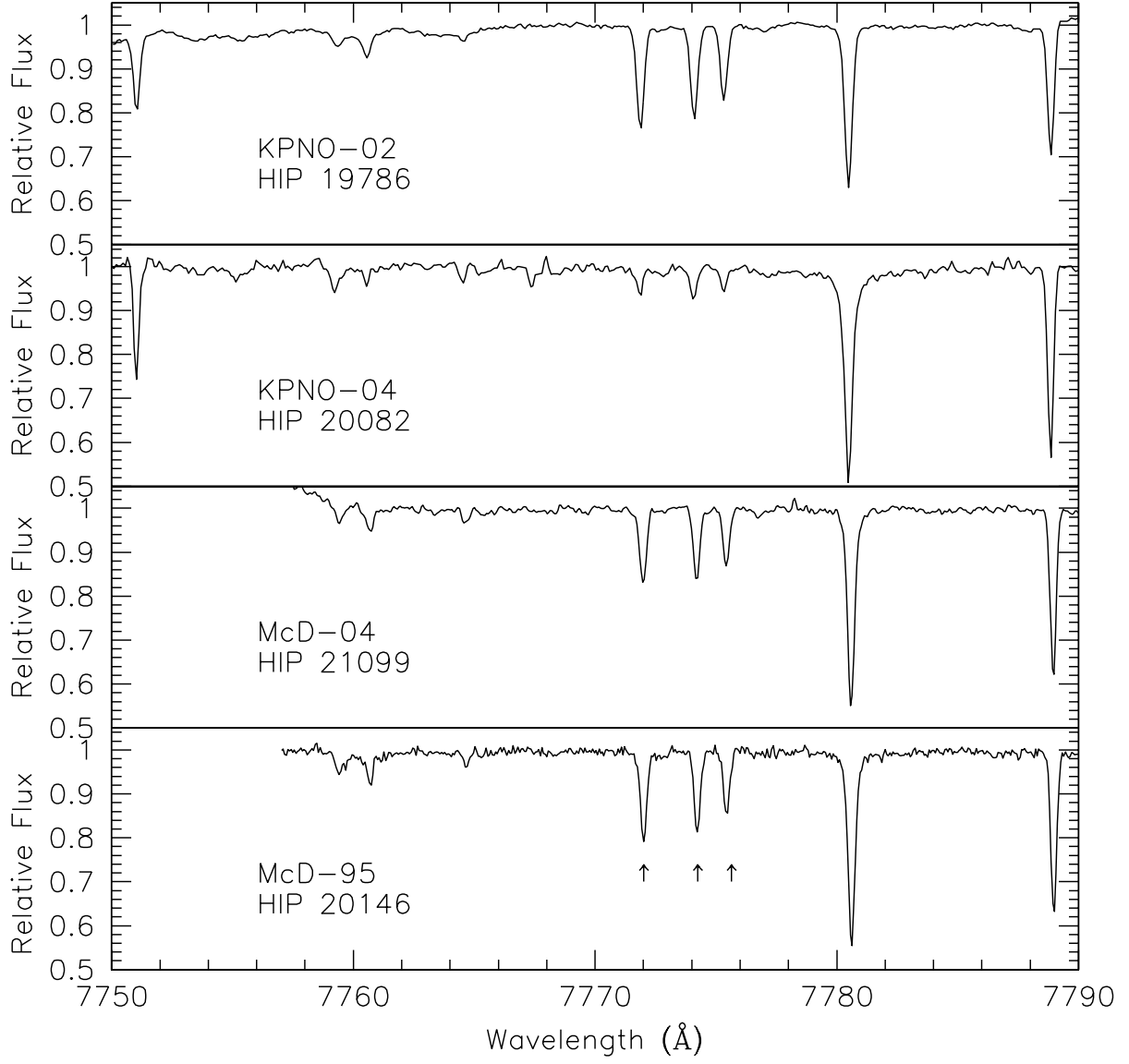


Fig. 1.— Sample high-resolution spectra of Hyades dwarfs from the Kitt Peak National Observatory 4-m and the McDonald Observatory 2.7-m telescopes. The source of each spectrum, as described in the text, is given, and the O I triplet is marked in the lower panel. Only the two reddest lines were measured for HIP 20082 ($T_{\text{eff}} = 4784$ K).

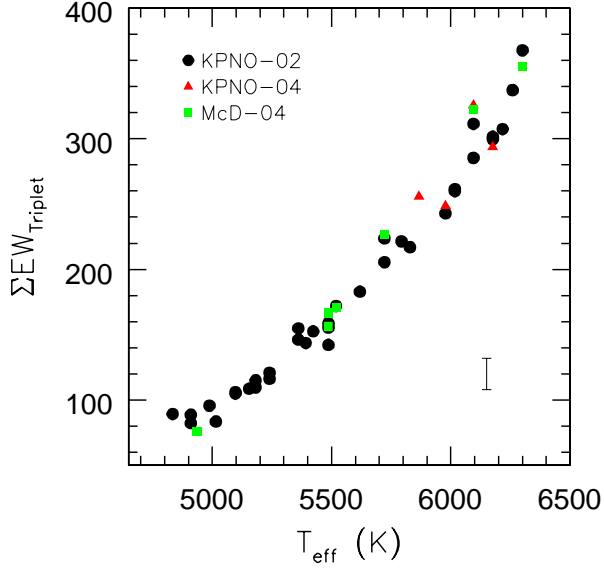


Fig. 2.— Sum of the triplet EWs as a function of T_{eff} for the combined Hyades data set. The points are distinguished by the data set from which they are measured. The vertical bar represents the 1σ uncertainty in the combined EWs. Only stars for which all three lines of the O I triplet are measurable are included.

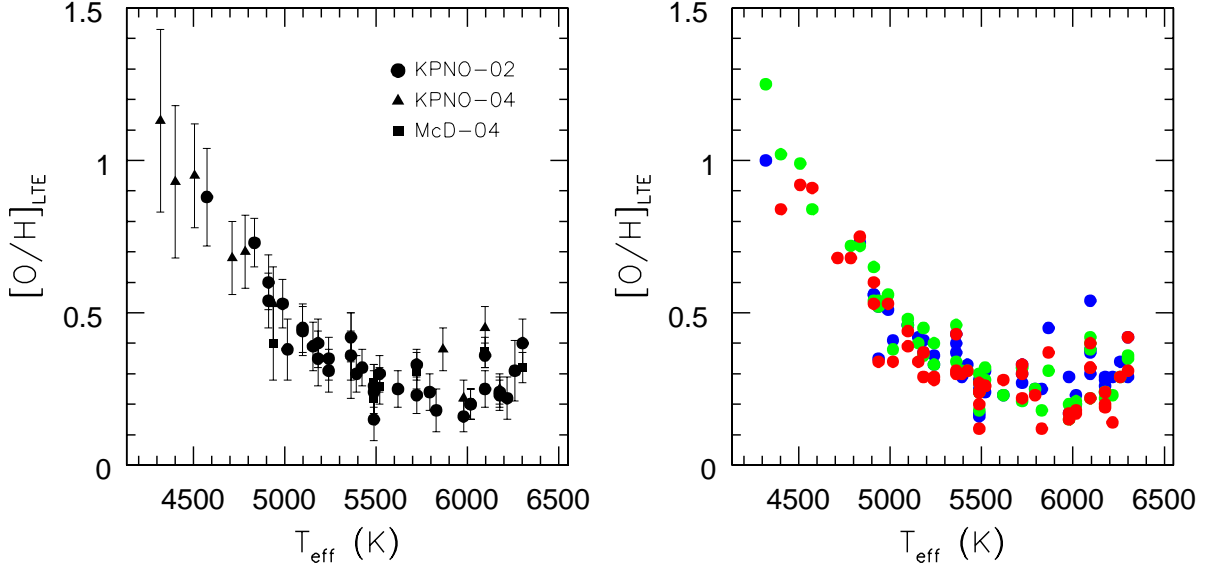


Fig. 3.— Left- Relative LTE O abundances vs. T_{eff} for the combined Hyades data set. The points are again distinguished by the data set from which they are derived. The error bars represent the total internal abundance uncertainties. Right- Line-by-line relative LTE O abundances vs. T_{eff} for the combined Hyades data set. Abundances derived from the $\lambda 7772$ line are given in blue, $\lambda 7774$ are green, and $\lambda 7775$ are red.

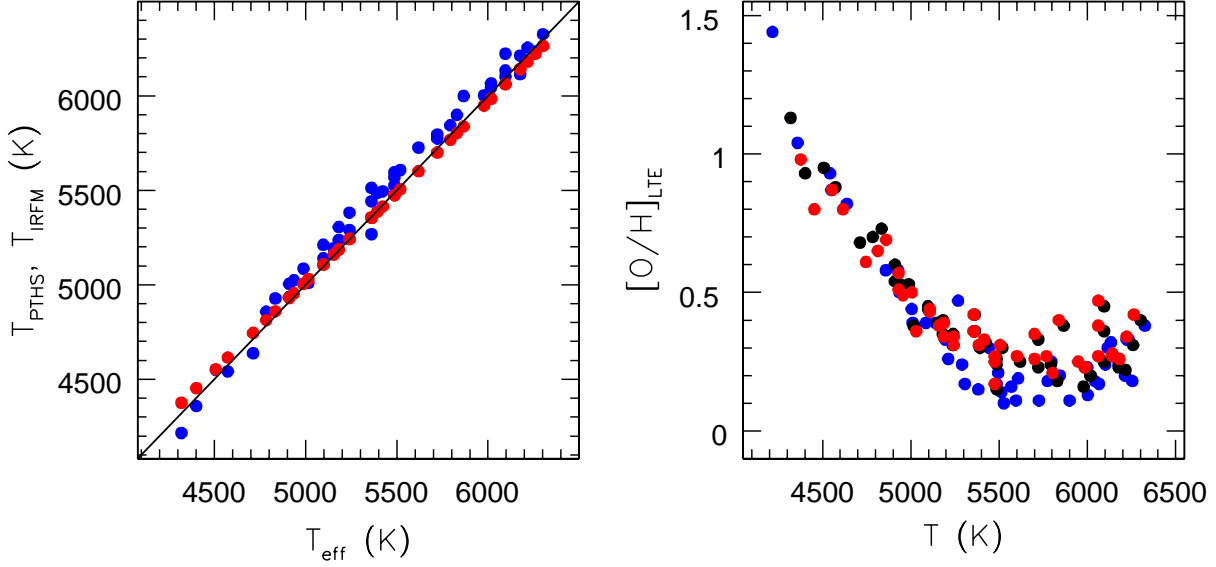


Fig. 4.— (a) Temperatures from the isochrone of Pinsonneault et al. (2004; blue) and from the metallicity-dependent temperature-color calibration of Ramírez & Meléndez (2005; red) vs. the adopted photometry-based temperatures. The diagonal line has a slope of unity and is the line of equality. (b) Relative LTE O abundances vs. temperature. Abundances derived using the adopted photometry-based temperatures (T_{eff}) are plotted in black, the Pinsonneault et al. isochrone-base temperatures (T_{PTHS}) in blue, and the Ramírez & Meléndez calibration-based temperatures (T_{IRFM}) in red. The sample has been trimmed of duplicates as described in the text.

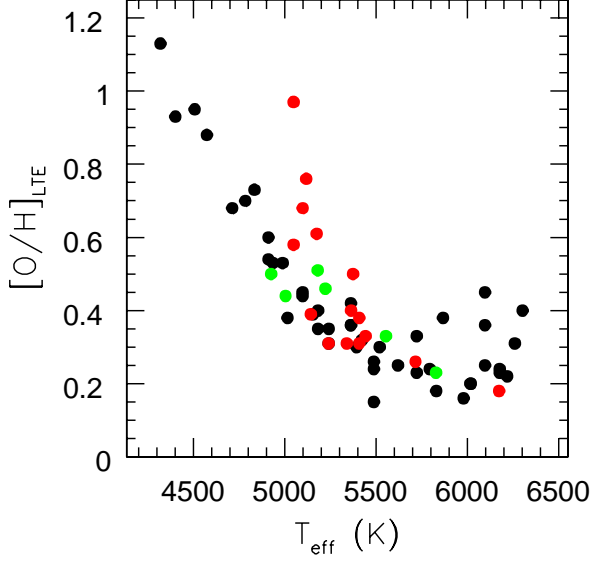


Fig. 5.— Hyades (black), Pleiades (red), and UMa (green) relative LTE O abundances vs. T_{eff} . The Hyades sample is trimmed of duplicates as described in the text. The Pleiades data are from SKHP, and the UMa data are from King & Schuler (2005)

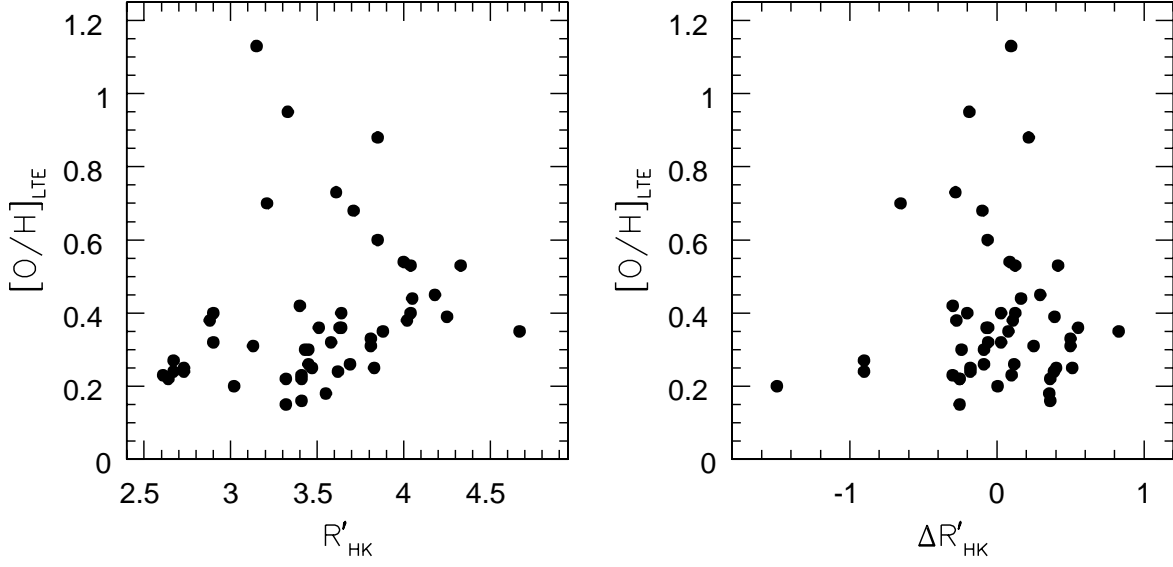


Fig. 6.— Left- Hyades relative LTE O abundances vs. Ca II H+K activity indicators. Activity data are from Paulson et al. (2002). Right- Hyades relative LTE O abundances vs. Ca II H+K activity residuals. The residuals are the difference in the observed and T_{eff} -dependent fitted values.

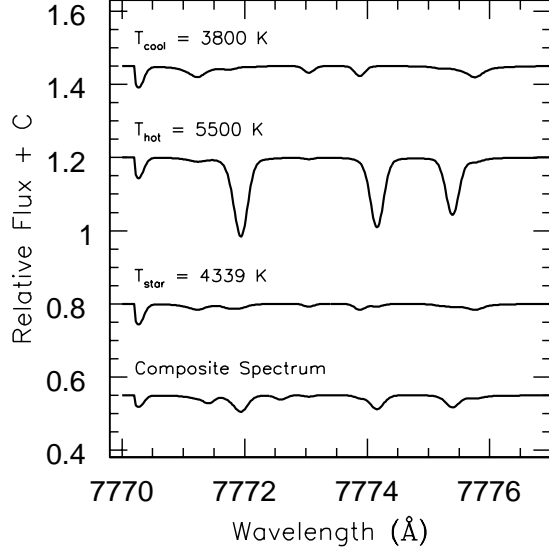


Fig. 7.— Synthesized component and composite spectra of HIP18322 used in the spot plausibility study. The spectra are synthesized with input O abundance of $[\text{O}/\text{H}] = +0.25$, the mean abundance of Hyads in the range $5450 \leq T_{\text{eff}} \leq 6100 \text{ K}$.

Table 1. Hyades Dwarfs Parameters

HIP	HD	$(B - V)$ (Mag)	Comment ^a	T_{eff} (K)	$\log g$ (cgs)	ξ (km s ⁻¹)	Telescope ^b
13806	...	0.86	P	5097	4.60	1.10	KPNO-02
13976	18632	0.93	P	4910	4.63	1.04	KPNO-02
14976	19902	0.73	A	5487	4.54	1.24	KPNO-02,McD-04
15310	20439	0.62	A	5866	4.47	1.40	KPNO-04
16529	...	0.84	A	5154	4.59	1.12	KPNO-02
16908	...	0.92	Y	4936	4.63	1.05	KPNO-04,McD-04
18322	286363	1.07	Y	4573	4.68	0.94	KPNO-02
18327	285252	0.90	P	4988	4.62	1.07	KPNO-02
18946	265348	1.10	Y	4507	4.69	0.92	KPNO-04
19098	285367	0.89	A	5015	4.61	1.08	KPNO-02
19148	25825	0.59	A	5978	4.44	1.45	KPNO-02,KPNO-04
19263	285482	1.01	Y	4712	4.66	0.98	KPNO-04
19441	...	1.19	Y	4319	4.72	0.87	KPNO-04
19781	26756	0.69	A	5619	4.51	1.30	KPNO-02
19786	26767	0.64	A	5793	4.48	1.37	KPNO-02
19793	26736	0.66	A	5722	4.49	1.34	KPNO-02,McD-04
19796	26784	0.51	A	6301	4.37	1.61	KPNO-02,McD-04
19934	284253	0.81	A	5240	4.58	1.15	KPNO-02
20082	285690	0.98	P	4784	4.65	1.00	KPNO-04
20130	27250	0.75	A	5423	4.55	1.22	KPNO-02
20146	27282	0.72	A	5519	4.53	1.26	KPNO-02,McD-95
20237	27406	0.56	A	6095	4.42	1.51	KPNO-02

Table 1—Continued

HIP	HD	$(B - V)$ (Mag)	Comment ^a	T_{eff} (K)	$\log g$ (cgs)	ξ (km s ⁻¹)	Telescope ^b
20480	27732	0.76	A	5392	4.55	1.21	KPNO-02
20492	27771	0.86	A	5097	4.60	1.10	KPNO-02
20557	27808	0.52	A	6259	4.38	1.59	KPNO-02
20712	28033	0.56	A	6095	4.42	1.51	KPNO-04,McD-04
20741	28099	0.66	A	5722	4.49	1.34	KPNO-02
20762	32347	1.15	Y	4401	4.70	0.89	KPNO-04
20815	28205	0.54	A	6176	4.40	1.55	KPNO-02
20826	28237	0.56	A	6095	4.42	1.51	KPNO-02
20827	285830	0.93	P	4910	4.63	1.04	KPNO-02
20949	283704	0.77	A	5361	4.56	1.20	KPNO-02
20951	285773	0.83	P	5182	4.59	1.13	KPNO-02
21099	28593	0.73	A	5487	4.54	1.24	KPNO-02,McD-04
21112	28635	0.54	A	6176	4.40	1.55	KPNO-02,KPNO-04
21317	28992	0.63	A	5829	4.47	1.39	KPNO-02
21637	29419	0.58	A	6017	4.43	1.47	KPNO-02
21741	284574	0.81	A	5240	4.58	1.15	KPNO-02
22380	30505	0.83	A	5182	4.59	1.13	KPNO-02
22422	30589	0.58	A	6017	4.43	1.47	KPNO-02
22566	30809	0.53	A	6217	4.39	1.57	KPNO-02
23312	...	0.96	P	4834	4.64	1.02	KPNO-02
23498	...	0.77	A	5361	4.56	1.20	KPNO-04
23750	240648	0.73	A	5487	4.54	1.24	KPNO-02

Table 1—Continued

HIP	HD	$(B - V)$ (Mag)	Comment ^a	T_{eff} (K)	$\log g$ (cgs)	ξ (km s ⁻¹)	Telescope ^b
24923	242780	0.77	A	5361	4.56	1.20	KPNO-02
Sun				5777	4.44	1.38	KPNO-02,KPNO-04,McD-04

^aProvides the source of the $(B - V)$ values: A- Allende Prieto & Lambert 1999; P- Paulson et al. 2003; Y- Yong et al. 2004

^bDenotes with which telescope the object was observed, as described in §2: KPNO-02- KPNO 4-m 2002; KPNO-04- KPNO 4-m 2004; McD-95- McDonald Observatory 2.7-m 1995; McD-04- McDonald Observatory 2.7-m 2004

Table 2. Triplet Equivalent Widths: KPNO-02

HIP	Blue Order				Red Order				Mean		
	S/N	EW ₇₇₇₂ (mÅ)	EW ₇₇₇₄ (mÅ)	EW ₇₇₇₅ (mÅ)	S/N	EW ₇₇₇₂ (mÅ)	EW ₇₇₇₄ (mÅ)	EW ₇₇₇₅ (mÅ)	EW ₇₇₇₂ (mÅ)	EW ₇₇₇₄ (mÅ)	EW ₇₇₇₅ (mÅ)
13806	290	38.1	36.0	29.7	194	44.5	36.5	27.2	41.3	36.3	28.5
13976	490	30.7	30.0	21.9	320	34.4	25.9	21.6	32.6	28.0	21.8
14976	340	57.8	54.5	42.6	260	65.2	51.2	39.5	61.5	52.9	41.1
16529	265	41.4	40.1	28.8	200	45.8	34.4	26.7	43.6	37.3	27.8
18322	245	...	18.8	16.2	170	...	18.4	15.5	...	18.6	15.9
18327	295	36.4	33.2	27.5	200	36.2	33.8	24.2	36.3	33.5	25.9
19098	208	32.6	28.0	21.5	195	34.7	29.0	21.3	33.7	28.5	21.4
19148	465	91.0	80.7	65.7	310	93.0	82.6	72.7	92.0	81.7	69.2
19781	300	65.7	64.9	51.5	218	71.8	57.3	54.7	68.8	61.1	53.1
19786	455	82.7	76.3	63.7	300	85.4	74.8	60.2	84.1	75.6	62.0
19793	405	82.0	80.6	63.2	295	87.3	70.1	64.2	84.7	75.4	63.7
19796	460	139.0	130.1	110.4	284	135.7	110.0	110.0	137.4	120.1	110.2
19934	293	44.4	39.6	32.6	190	46.5	40.9	28.5	45.5	40.3	30.6
20130	286	56.5	53.6	39.9	208	61.6	49.5	44.0	59.1	51.6	42.0
20146	289	61.8	61.5	46.5	194	71.1	57.5	45.6	66.5	59.5	46.1
20237	390	115.8	111.1	86.8	300	116.8	104.4	87.9	116.3	107.8	87.4
20480	275	50.7	49.4	38.7	186	58.6	49.6	40.4	54.7	49.5	39.6
20492	320	37.7	37.5	27.7	205	44.6	36.5	25.8	41.2	37.0	26.8
20557	355	129.0	118.6	96.8	298	125.4	106.3	98.5	127.2	112.4	97.7
20741	340	76.2	74.0	56.5	240	84.1	62.8	57.4	80.2	68.4	57.0

Table 2—Continued

HIP	Blue Order				Red Order				Mean		
	S/N	EW ₇₇₇₂ (mÅ)	EW ₇₇₇₄ (mÅ)	EW ₇₇₇₅ (mÅ)	S/N	EW ₇₇₇₂ (mÅ)	EW ₇₇₇₄ (mÅ)	EW ₇₇₇₅ (mÅ)	EW ₇₇₇₂ (mÅ)	EW ₇₇₇₄ (mÅ)	EW ₇₇₇₅ (mÅ)
20815	387	114.8	106.6	88.5	260	112.4	97.4	79.8	113.6	102.0	84.2
20826	390	107.0	98.3	80.2	270	113.5	91.6	80.2	110.2	95.0	80.2
20827	285	30.5	32.9	24.7	190	35.4	30.9	23.0	33.0	31.9	23.9
20949	238	55.4	56.9	40.0	180	57.1	53.3	47.0	56.3	55.1	43.5
20951	320	41.6	43.6	29.6	200	44.4	39.5	31.5	43.0	41.6	30.6
21099	325	53.7	47.1	39.9	220	55.5	52.4	35.7	54.6	49.8	37.8
21112	347	112.7	105.5	84.0	255	117.1	97.8	85.9	114.9	101.7	85.0
21317	230	84.9	76.5	60.6	180	87.6	70.1	54.1	86.3	73.3	57.4
21637	380	96.5	90.1	73.1	250	98.6	87.8	73.8	97.6	89.0	73.5
21741	343	46.5	44.1	33.1	196	47.2	42.4	28.5	46.9	43.3	30.8
22380	280	40.9	39.1	28.5	189	48.5	35.6	26.8	44.7	37.4	27.7
22422	349	98.7	89.6	71.4	256	100.7	87.8	74.9	99.7	88.7	73.2
22566	297	116.5	108.2	84.4	265	122.7	101.3	81.8	119.6	104.8	83.1
23312	256	30.1	30.9	24.5	162	39.6	29.2	24.4	34.9	30.1	24.5
23750	261	58.0	59.1	45.6	176	61.4	52.8	40.5	59.7	56.0	43.1
24923	274	56.7	48.6	38.1	163	63.6	48.5	37.0	60.2	48.6	37.6
Sun	342	64.3	61.0	50.3	219	68.8	58.7	47.5	66.6	59.9	48.9

Table 3. Triplet Equivalent Widths: KPNO-04 & McDonald

HIP	S/N	EW ₇₇₇₂ (mÅ)	EW ₇₇₇₄ (mÅ)	EW ₇₇₇₅ (mÅ)
KPNO-04				
15310	142	103.4	82.5	69.9
16908	210	31.8	28.2	...
18946	206	...	18.2	11.9
19148	125	100.0	83.4	65.1
19263	188	14.9
19441	212	11.0	13.2	...
20082	221	...	25.8	18.0
20712	123	130.4	108.0	87.4
20762	220	...	12.8	6.9
21112	139	114.1	97.9	81.7
23498	85	56.9	...	34.7
Sun	272	65.6	58.0	44.4
McDonald				
14976	237	67.0	55.2	44.1
16908	131	29.8	28.7	17.6
19793	184	88.7	76.2	61.4
19796	208	133.0	121.5	100.7
20712	131	125.9	109.5	87.2
21099	190	60.3	53.4	42.6
20146 ^a	234	67.2	58.1	45.6
Sun	825	72.8	60.2	48.2

^aObserved with the McDonald Observatory
2.7-m telescope in 1995

Table 4. Oxygen Triplet Abundances and Uncertainties

HIP	[O/H]	σ
KPNO-02 ^a		
13806	0.45	± 0.08
13976	0.54	± 0.09
14976	0.24	± 0.07
16529	0.39	± 0.08
18322	0.88	± 0.16
18327	0.53	± 0.08
19098	0.38	± 0.10
19148	0.16	± 0.05
19781	0.25	± 0.06
19786	0.24	± 0.06
19793	0.33	± 0.05
19796	0.40	± 0.08
19934	0.31	± 0.07
20130	0.32	± 0.06
20146	0.30	± 0.06
20237	0.36	± 0.04
20480	0.30	± 0.06
20492	0.44	± 0.08
20557	0.31	± 0.10
20741	0.23	± 0.06
20815	0.23	± 0.05
20826	0.25	± 0.06
20827	0.60	± 0.09
20949	0.42	± 0.08
20951	0.40	± 0.08
21099	0.15	± 0.07
21112	0.24	± 0.05
21317	0.18	± 0.07

Table 4—Continued

HIP	[O/H]	σ
21637	0.20	± 0.05
21741	0.35	± 0.07
22380	0.35	± 0.09
22422	0.20	± 0.05
22566	0.22	± 0.07
23312	0.73	± 0.08
23750	0.26	± 0.07
24923	0.36	± 0.08
KPNO-04		
15310	0.38	± 0.07
16908	0.53	± 0.12
18946	0.95	± 0.17
19148	0.22	± 0.06
19263	0.68	± 0.12
19441	1.13	± 0.30
20082	0.70	± 0.12
20712	0.45	± 0.07
20762	0.93	± 0.25
21112	0.25	± 0.05
23498	0.36	± 0.14
McDonald		
14976	0.27	± 0.06
16908	0.40	± 0.12
19793	0.31	± 0.06
19796	0.32	± 0.05
20712	0.37	± 0.05
21099	0.22	± 0.06

Table 4—Continued

HIP	[O/H]	σ
20146	0.26	± 0.06

^aKPNO-02 abundances are those derived using the mean EWs.

Table 5. Line-by-line Triplet Abundance Sensitivities

HIP	Parameter	Abundance Sensitivity		
		7772	7774	7775
21112 ($T_{\text{eff}} = 6176$ K)	$\Delta T_{\text{eff}} = \pm 150$ K	∓ 0.11	∓ 0.12	∓ 0.12
	$\Delta \log g = \pm 0.25$ dex	± 0.04	± 0.06	± 0.07
	$\Delta \xi = \pm 0.30$ km s ⁻¹	∓ 0.04	∓ 0.04	∓ 0.04
19786 ($T_{\text{eff}} = 5793$ K)	$\Delta T_{\text{eff}} = \pm 150$ K	∓ 0.15	∓ 0.15	∓ 0.15
	$\Delta \log g = \pm 0.25$ dex	$^{+0.08}_{-0.03}$	$^{+0.09}_{-0.04}$	$^{+0.09}_{-0.05}$
	$\Delta \xi = \pm 0.30$ km s ⁻¹	∓ 0.03	∓ 0.03	∓ 0.03
20082 ($T_{\text{eff}} = 4784$ K)	$\Delta T_{\text{eff}} = \pm 150$ K	\cdots	$^{-0.23}_{+0.27}$	$^{-0.23}_{+0.27}$
	$\Delta \log g = \pm 0.25$ dex	\cdots	$^{+0.05}_{-0.08}$	$^{+0.06}_{-0.09}$
	$\Delta \xi = \pm 0.30$ km s ⁻¹	\cdots	∓ 0.01	∓ 0.01

Table 6. Comparison of Oxygen Abundances

HIP	KPNO-02		KPNO-04		McD-04	
	[O/H]	σ	[O/H]	σ	[O/H]	σ
14976	0.24	± 0.07	0.27	± 0.06
16908	0.53	± 0.12	0.40	± 0.12
19148	0.16	± 0.05	0.22	± 0.06
19793	0.33	± 0.05	0.31	± 0.06
19796	0.40	± 0.08	0.32	± 0.05
20146	0.30	± 0.06	0.26	± 0.06
20712	0.45	± 0.07	0.37	± 0.05
21099	0.15	± 0.07	0.22	± 0.06
21112	0.24	± 0.05	0.25	± 0.05

Table 7. Spot Synthesis Results

HIP	T_{eff} (K)	T_{cool} (K)	T_{hot} (K)	T_{star} (K)	Observed			Composite		
					EW_{7771} (mÅ)	EW_{7774} (mÅ)	EW_{7775} (mÅ)	EW_{7771} (mÅ)	EW_{7774} (mÅ)	EW_{7775} (mÅ)
18327	4988	4200	5900	4785	36.3	33.5	25.9	39.9	32.3	27.1
20082	4784	4000	5700	4569	...	25.8	18.0	...	25.1	21.4
18322	4573	3800	5500	4339	...	18.6	15.9	...	19.6	17.3